Journal of Macromolecular Science, Part A
Publication details, including instructions for authors and subscription information:
http://www.informaworld.com/smpp/title~content=t713597274

Observation of a Silk-Like Crystal Structure in a Genetically Engineered Periodic Polypeptide

Mark T. Krejchi[a]; Edward D. T. Atkins[b]; Maurille J. Fournier[c]; Thomas L. Mason[c]; David A. Tirrell[a]
[a] Department of Polymer Science and Engineering, University of Massachusetts Amherst, Massachusetts, USA [b] H. H. Wills Physics Laboratory, University of Bristol, Bristol, UK [c] Department of Biochemistry and Molecular Biology, University of Massachusetts Amherst, Massachusetts, USA

To cite this Article Krejchi, Mark T. , Atkins, Edward D. T. , Fournier, Maurille J. , Mason, Thomas L. and Tirrell, David A.(1996) 'Observation of a Silk-Like Crystal Structure in a Genetically Engineered Periodic Polypeptide', Journal of Macromolecular Science, Part A, 33: 10, 1389 — 1398
To link to this Article: DOI: 10.1080/10601329608014915
URL: http://dx.doi.org/10.1080/10601329608014915

J.M.S.—PURE APPL. CHEM., A33(10), pp. 1389–1398 (1996)

OBSERVATION OF A SILK-LIKE CRYSTAL STRUCTURE IN A GENETICALLY ENGINEERED PERIODIC POLYPEPTIDE

MARK T. KREJCHI

Department of Polymer Science and Engineering
University of Massachusetts
Amherst, Massachusetts 01003, USA

EDWARD D. T. ATKINS

H. H. Wills Physics Laboratory
University of Bristol
Bristol BS8 1TL, UK

MAURILLE J. FOURNIER AND THOMAS L. MASON

Department of Biochemistry and Molecular Biology
University of Massachusetts
Amherst, Massachusetts 01003, USA

DAVID A. TIRRELL*

Department of Polymer Science and Engineering
University of Massachusetts
Amherst, Massachusetts 01003, USA

ABSTRACT

A genetically engineered periodic polypeptide consisting of 36 repeats of the octapeptide sequence -(AlaGly)$_3$GluGly- has been crystallized from solution in aqueous lithium bromide. Analysis by solid-state nuclear magnetic resonance spectroscopy, vibrational spectroscopy, and wide-angle x-ray diffraction reveals a crystal structure analogous to that

obtained when silk solutions are allowed to dry under quiescent conditions, i.e., the silk I structure. Previous analyses of the same polymer have demonstrated an antiparallel β-sheet architecture (silk II structure) in samples crystallized from formic acid. These results illustrate the potential for controlling the solid-state structures and properties of genetically engineered materials through selection of appropriate processing and crystallization conditions.

INTRODUCTION

Recent developments in the bacterial expression of artificial genes have given rise to a new class of polymeric materials characterized by essentially uniform macromolecular architectures [1–8]. Our interest in such materials has been directed in part toward the engineering of controlled crystal structures, and we have recently reported the synthesis and solid-state structural analysis of the repetitive polypeptide comprising 36 copies of octapeptide **1** [8d].

-(AlaGly)$_3$GluGly- **1**

The design of sequence **1** has been described in detail [8d]. A key element of the design was the known propensity of poly(L-alanylglycine) [poly(AG)] and *Bombyx mori* silk fibroin to adopt antiparallel (ap)β-sheet structures in the solid state. Glutamic acid was inserted into the sequence at intervals of eight amino acids in order to 1) define the folding periodicity of the chain, and 2) control the chemical functionality of the surfaces of the resulting lamellar crystals. The key elements of the expected structure have been verified in polymers of **1** crystallized from formic acid, with the anticipated apβ-architecture supported by the results of x-ray diffraction and spectroscopic analyses.

But poly(AG) and *B. mori* fibroin are known to exhibit a second crystal structure as well. Designated silk I, this structure is observed when silk solutions are allowed to dry under quiescent conditions, or when poly(AG) is isolated by dialysis from solutions in aqueous lithium bromide. The silk I structure is unstable with respect to conversion to the β (silk II) form, and it has been described by Lotz and Keith [9] as a "crankshaft" architecture with glycine and alanine residues adopting dihedral angles that approximate those of α-helical and extended conformations, respectively. Alternative structures have also been proposed for silk I [10].

Our previous work on polymers of **1** was directed toward the growth of macromolecular crystals consisting of stacked, folded β-sheets [8d]. We show herein that such polymers can be obtained in a silk I-like architecture as well, through selection of appropriate crystallization conditions.

EXPERIMENTAL

Polymer Synthesis

The biological synthesis and molecular characterization of the polymer used in this work [designated poly(AG)$_3$EG] [11] have been described in detail [8d]. All of the analytical results are consistent with a structure comprising 36 repeats of sequence **1**.

Crystallization from Aqueous Lithium Bromide

Crystallization from aqueous lithium bromide was carried out by using a standard procedure developed for the preparation of the silk I-like form of poly-(AG) [12]. Powder samples were prepared by dissolving the polymer in 60% aqueous lithium bromide and dialyzing this solution against progressively diluted solutions of lithium bromide. A precipitate developed at a lithium bromide concentration of 12%, but the dilution process was continued until all the lithium bromide was removed. The precipitate was collected by centrifugation, washed with methanol, and dried overnight in vacuo at room temperature. Only 32% of the original sample weight was recovered in this process, the remaining being precipitated by the addition of methanol. The total recovery using this procedure was approximately 87%. CP/MAS ^{13}C-NMR, and Raman spectroscopic analysis (not shown) indicated both precipitates were identical; however, only the fraction recovered by dialysis against progressively diluted solutions of lithium bromide was characterized in detail. This fraction is designated poly(AG)$_3$EG-I.

Crystallization from Formic Acid

Poly(AG)$_3$EG was crystallized from formic acid as described in Ref. 8d. The resulting sample is designated poly(AG)$_3$EG-II.

Measurements

Infrared and Raman spectra were obtained on IBM IR32 Fourier Transform Infrared and Bruker FRA 106 Fourier Transform Raman spectrophotometers, respectively. Cross polarization/magic angle spinning ^{13}C-NMR spectra were obtained at 50 MHz on powder samples using a Bruker 200AC spectrometer equipped with a DOTY solids probe and an IBM solids rack. Measurements were collected at a spinning speed of ca. 4000 Hz with a 5-μs 90°pulse and a cross-polarization time of 2 ms. A line broadening factor of 50 was used during data processing. X-ray diffraction patterns were obtained with a Statton-type evacuated x-ray camera. The nickel-filtered CuKα sealed beam source was collimated with a system of 200-μm pinholes. Poly(AG)$_3$EG-I was examined as a powder enclosed in a thin-wall glass capillary.

RESULTS AND DISCUSSION

CP/MAS Solid-State ^{13}C-NMR Spectroscopy

The similarity of the structure of poly(AG)$_3$EG-I to that of silk I [and poly-(AG)-II] is shown most clearly by solid-state ^{13}C-NMR spectroscopy. Figure 1 shows the CP/MAS ^{13}C-NMR spectra of poly(AG)$_3$EG as crystallized from formic acid and aqueous LiBr, respectively. The observed chemical shifts and assignments for the alternative structures of silk, poly(AG) and poly(AG)$_3$EG are summarized in Table 1.

The resonance frequencies observed for the glycine and alanine carbons of poly(AG)$_3$EG-I are essentially identical to those of silk I and poly(AG)-II, and quite

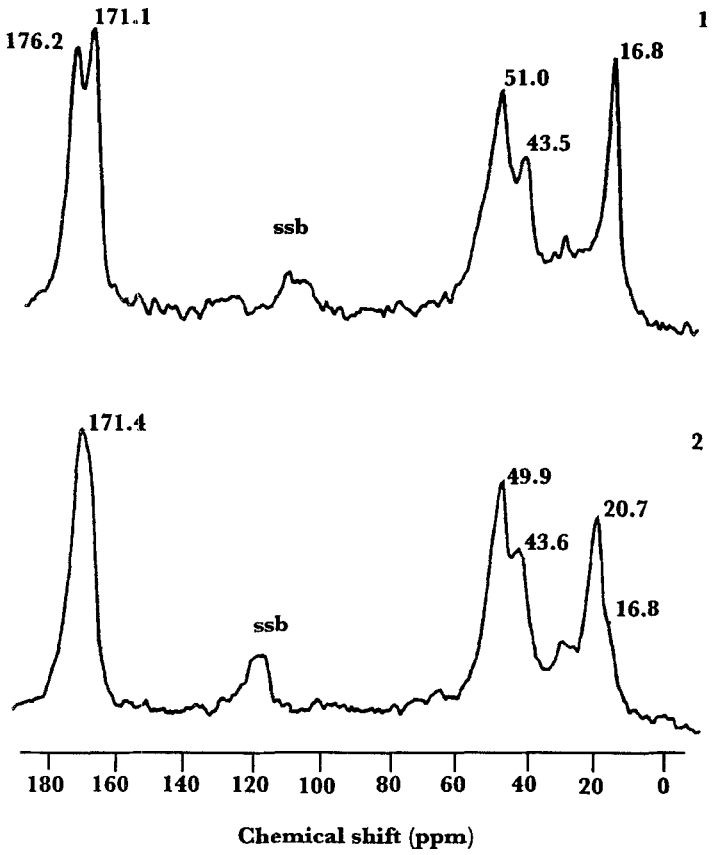

FIG. 1. CP/MAS ^{13}C-NMR spectra of (1) poly(AG)$_3$EG-I and (2) poly(AG)$_3$EG-II.

TABLE 1. Chemical Shifts and Assignments of Signals Observed in the CP/MAS ^{13}C-NMR Spectra of Silk [13], Poly(AG) [13], and Poly(AG)$_3$EG

	Chemical shift, ppm					
Carbon	Poly(AG)$_3$EG-I	Silk I	Poly(AG)-II	Poly(AG)$_3$EG-II	Silk II	Poly(AG)-I
Ala C_α	51.0	50.3	50.5	49.9	48.8	48.5
Ala C_β	16.8	16.6	16.6	20.7	19.2	20.0
Ala C=O	176.2	177.5	177.1	171.4	171.5	171.8
Gly C_α	43.5	43.9	43.7	43.6	43.1	43.3
Gly C=O	171.1	171.1	171.9	171.4	169.8	168.4

distinct from those of the β-forms of poly(AG)$_3$EG [8d], silk [13], and poly(AG) [13]. Particularly diagnostic are the β- and carbonyl carbons of alanine, which are shifted by 4–6 ppm in the two alternative crystal structures. The β-carbon of alanine in poly(AG)$_3$EG-I lies at 16.8 ppm, nearly coincident with that of silk I, which appears at 16.6 ppm [13]. The absence of a shoulder at 20.7 ppm indicates that the sample contains little, if any, of the β-form of poly(AG)$_3$EG. The alanine carbonyl resonance at 176.2 ppm is also diagnostic for the silk I structure, as the corresponding signal in the β-form lies at 171.4 ppm.

Vibrational Spectroscopy

The infrared spectra obtained from poly(AG)$_3$EG-I and poly(AG)$_3$EG-II are shown in Fig. 2. There are substantial differences in the frequencies and intensities of the bands observed in polymers crystallized from formic acid and from aqueous lithium bromide. The amide A, amide I, and amide II vibrational modes are observed at 3289, 1652, and 1538 cm^{-1}, respectively, in poly(AG)$_3$EG-I, and at 3286, 1623, and 1521 cm^{-1} respectively, in poly(AG)$_3$EG-II. The absence of the characteristic amide I band at ca. 1625 cm^{-1} confirms that poly(AG)$_3$EG-I contains little of the β-form.

The Raman spectra obtained from poly(AG)$_3$EG-I and poly(AG)$_3$EG-II are shown in Fig 3. As in the infrared analysis, comparison of these spectra reveals substantial differences in the frequencies and intensities of the bands observed in

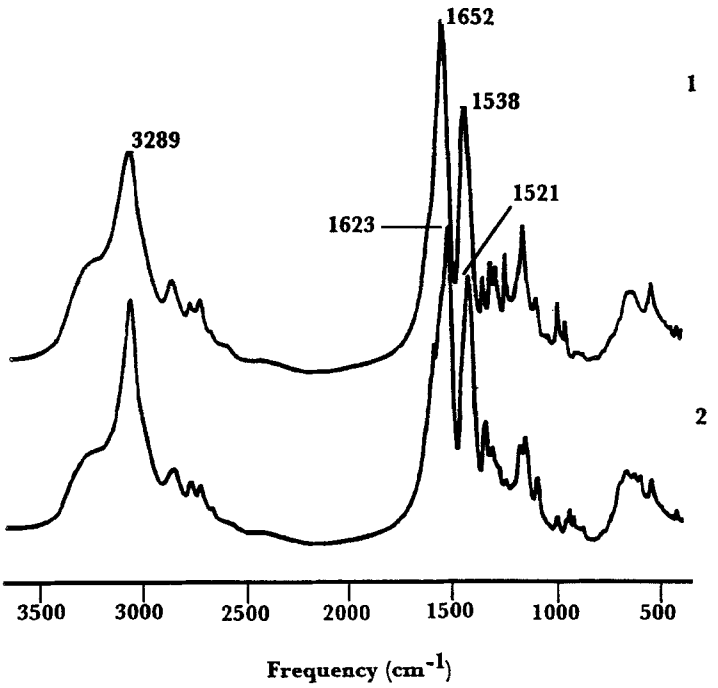

FIG. 2. Infrared spectra of (1) poly(AG)$_3$EG-I and (2) poly(AG)$_3$EG-II.

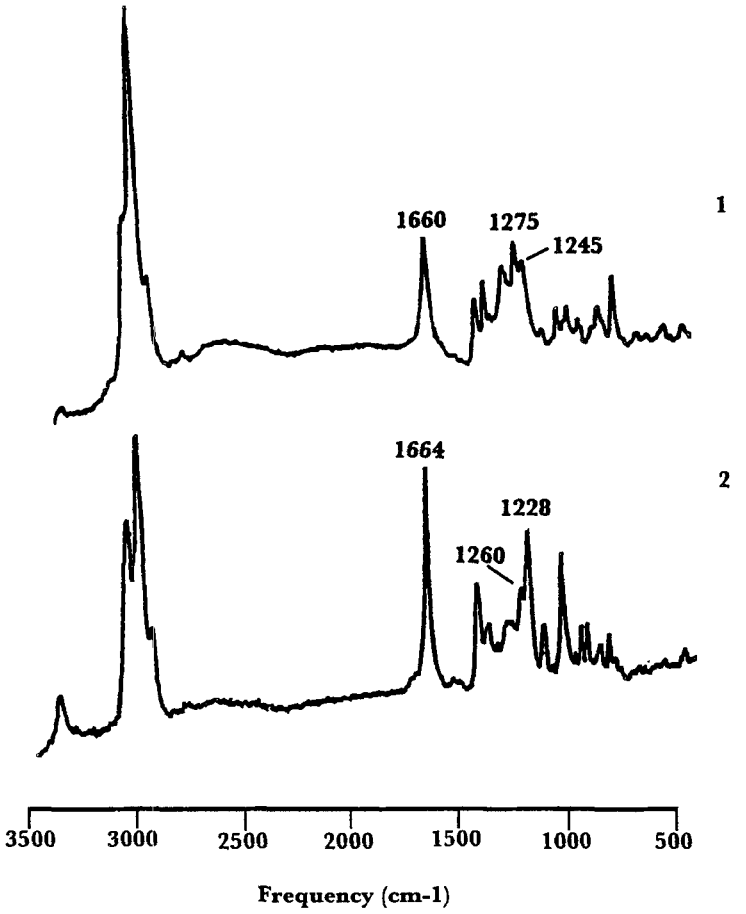

FIG. 3. Raman spectra of (1) poly(AG)$_3$EG-I and (2) poly(AG)$_3$EG-II.

poly(AG)$_3$EG-I and poly(AG)$_3$EG-II. The main amide I band at 1660 cm^{-1} in poly(AG)$_3$EG-I suggests a dominant structure different from the apβ-sheet, which is characterized by a sharp amide I absorption at 1664 cm^{-1} [8d].

X-Ray Diffraction

Wide-angle diffraction patterns of poly(AG)EG-I were obtained as powders; a representative example is shown in Fig. 4. A wide-angle diffraction pattern obtained from a powder sample of poly(AG)$_3$EG-II is included for comparison. Even a qualitative examination of Fig. 4 indicates that the structure of poly(AG)$_3$EG-I is different from that of P(AG)$_3$EG-II, in accord with the spectroscopic results discussed previously. The differences may be rationalized on the basis of a chain axis contraction in P(AG)$_3$EG-I, similar to that proposed by Lotz and coworkers for poly(AG)-II [9]. On the basis of this argument, the diffraction pattern of poly-(AG)$_3$EG-I was indexed on an orthorhombic unit cell with dimensions a = 0.948 nm, b = 1.734 nm, and c (chain axis) = 0.940 nm (errors ± 0.002 nm). The mea-

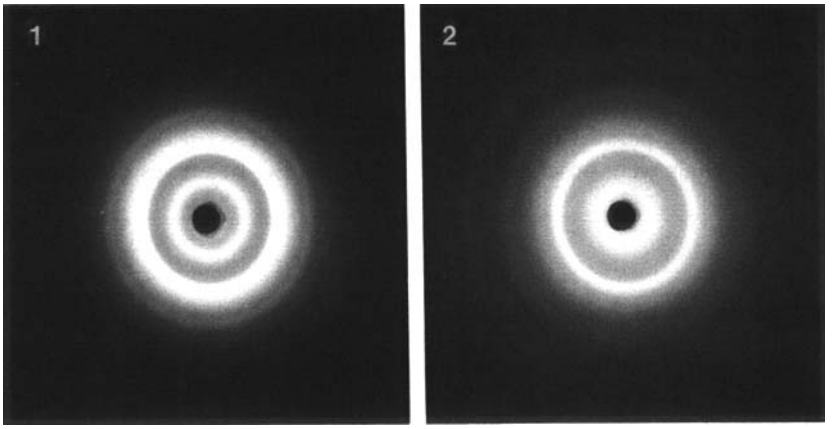

FIG. 4. Wide-angle x-ray diffraction patterns from powders of (1) poly$(AG)_3$EG-I and (2) poly$(AG)_3$EG-II.

sured and calculated interplanar spacings are in good agreement, and indexing details are listed in Table 2. The value of the 0.948-nm spacing was assigned on the basis of its second diffraction order at 0.474 nm. This diffraction signal is also observed in poly$(AG)_3$EG-II and, in both cases, is attributed to the distance between hydrogen-bonded chains. The value of 1.734 nm for b, or more specifically its second diffraction order observed at 0.87 nm, represents the average intersheet stacking periodicity. This value is 21% greater than the value reported for poly(AG)-II (0.72 nm) [9]; the same percentage difference in spacing is observed for the diffraction signals indexed 020 in poly$(AG)_3$EG-II and in poly(AG)-I [8d].

The direct determination of the 001 spacing was not possible, as this diffraction signal and all of its higher orders are obstructed by other hkl signals observed in the powder patterns of poly$(AG)_3$EG-I. As a result, the c-axis dimension of 0.940 nm was determined from the diffraction signal indexed 211. This diffraction signal, although shifted to a lower angle, is similar in character to the signal indexed

TABLE 2. Comparison of the Observed Diffraction Signal Spacings (d_0) in Poly$(AG)_3$EG-I with Those Calculated (d_c) for an Orthorhombic Unit Cell With Dimensions a = 0.948 nm, b = 1.734 nm, c = 0.940 nm (errors ± 0.002 nm)

	kl	d_0	d_c		kl	d_0	d_c
$h = 0$	10	1.734	1.734	$h = 3$	10	0.324	0.311
	20	0.867	0.867		11	0.290	0.295
$h = 2$	00	0.474	0.474		22	0.259	0.251
	10	0.461	0.457	$h = 4$	00	0.238	0.237
	11	0.411	0.411		10	0.234	0.234
					11	0.226	0.227
					22	0.205	0.205

equivalently in poly$(AG)_3$EG-II, suggesting that the coherence length in the *c* dimension is small compared to the other crystallographic dimensions [8d]. Although the positions of the observed diffraction signals in poly$(AG)_3$EG-I make it difficult to establish a hierarchy of coherent scattering lengths in the *a*, *b*, and *c* directions, it is assumed that they parallel the order observed in poly$(AG)_3$EG-II. No low angle diffraction signals were observed in any poly$(AG)_3$EG-I samples prepared in this work.

Crystal Structure of Poly$(AG)_3$EG-I

Based on the previous detailed analysis of the solid-state structure of poly-$(AG)_3$EG [8d], the experimental evidence collected on the solid-state structure of poly$(AG)_3$EG-I supports a crystalline sheet architecture involving a chain-folded lamellar structure as the basic crystalline unit. The powder x-ray diffraction patterns we have obtained for poly$(AG)_3$EG-I do not provide sufficient information for us to determine a detailed structure, or to delineate clearly between previously proposed models for silk I or poly(AG)-II. The only x-ray structure determination that has been attempted for poly(AG)-II is that of Lotz and Keith [9]. If we assume that our poly$(AG)_3$EG-I structure is similar, then it would be envisaged to be constructed by contracting the traditional apβ-sheet structure by allowing alternative amino acid residues to adopt conformations such that successive peptide groups are aligned approximately parallel and perpendicular to the chain axis. Lotz and coworkers refer to this chain arrangement as a "crankshaft" conformation. Such an arrangement results in a peptide backbone that is highly contracted such that the rise per amino acid residue is 0.24 nm in poly$(AG)_3$EG-I compared to 0.35 nm in poly$(AG)_3$EG-II. This *c*-axis contraction [identical to that reported by Lotz and coworkers for poly(AG)-II] leads to an expansion in the *b* dimension, resulting in the increased intersheet spacing observed in poly$(AG)_3$EG-I. Lamellar crystals that form the basis of this crystalline entity are constructed from the lateral stacking of sheets as in poly$(AG)_3$EG-II. As in the model proposed by Lotz and coworkers, there are four amino acid residues per chain axis repeat related by a 2-fold screw axis. The alanine residues adopt dihedral angles that approximate an extended β-type conformation, and glycine residues are configured as left-handed α-helices. As a result of the absence of any low-angle signals in the x-ray diffraction patterns of poly$(AG)_3$EG-I, no statements regarding the specific details of chain folding can be made.

ACKNOWLEDGMENTS

We thank S. L. Hsu for guidance in vibrational spectroscopy, and L. K. Thompson for help in obtaining solid-state NMR spectra. This work was supported by grants from the Polymers and Genetics Programs of the National Science Foundation, and by the NSF Materials Research Science and Engineering Center at the University of Massachusetts.

REFERENCES AND NOTES

[1] J. Cappello and F. Ferrari, in *Plastics from Microbes: Microbial Synthesis of Polymers and Polymer Precursors* (D. P. Mobley, Ed.), Hanser/Gardner Publications, Munich, 1994, p. 35.

[2] S. T. Case, J. Powers, R. Hamilton, and M. J. Burton, in *Silk Polymers* (D. Kaplan, W. W. Adams, B. Farmer, and C. Viney, Eds.), American Chemical Society, Washington, D.C., 1994, p. 81.

[3] I. Goldberg and A. J. Salerno, in *Materials Synthesis Utilizing Biological Processes* (P. C. Reike, P. D. Calvert, and M. Alper, Eds.), Materials Research Society, Pittsburgh, PA, 1990, p. 229.

[4] D. T. McPherson, C. Morrow, D. S. Minehan, J. Wu, E. Hunter, and D. W. Urry, *Biotechnol. Prog., 8*, 347 (1992).

[5] A. J. Salerno and I. Goldberg, *Appl. Microbiol. Biotechnol., 58*, 209 (1993).

[6] J. P. O'Brien, R. H. Hoess, K. H. Gardner, R. L. Lock, Z. R. Wasserman, P. C. Weber, and F. R. Salemme, in *Silk Polymers* (D. Kaplan, W. W. Adams, B. Farmer, and C. Viney, Eds.), American Chemical Society, Washington, D.C., 1994, p. 104.

[7] K. P. McGrath and D. L. Kaplan, in *Biomolecular Materials* (C. Viney, S. T. Case, and J. H. Waite, Eds.), Materials Research Society, Pittsburgh, PA, 1993, p. 83.

[8] (a) K. P. McGrath, M. J. Fournier, T. L. Mason, and D. A. Tirrell, *J. Am. Chem. Soc., 114*, 727 (1992). (b) H. S. Creel, M. J. Fournier, T. L. Mason, and D. A. Tirrell, *Macromolecules, 24*, 1213 (1991). (c) G. Zhang, M. J. Fournier, T. L. Mason, and D. A. Tirrell, *Ibid., 25*, 3601 (1992). (d) M. T. Krejchi, E. D. T. Atkins, A. J. Waddon, M. J. Fournier, T. L. Mason, and D. A. Tirrell, *Science, 265*, 1427 (1994). (e) R. C. Beavis, B. T. Chait, H. S. Creel, M. J. Fournier, T. L. Mason, and D. A. Tirrell, *J. Am. Chem. Soc., 114*, 7584 (1992). (f) E. Yoshikawa, M. J. Fournier, T. L. Mason, and D. A. Tirrell, *Macromolecules, 27*, 5471 (1994). (g) S. Kothakota, T. L. Mason, D. A. Tirrell, and M. J. Fournier, *J. Am. Chem. Soc., 117*, 536 (1995). (h) Y. Deguchi, M. J. Fournier, T. L. Mason, and D. A. Tirrell, *J. Macromol. Sci.—Pure Appl. Chem., A31*, 1691 (1994). (i) M. J. Dougherty, S. Kothakota, T. L. Mason, D. A. Tirrell, and M. J. Fournier, *Macromolecules, 26*, 1779 (1993).

[9] B. Lotz and H. D. Keith, *J. Mol. Biol., 61*, 201 (1971).

[10] (a) T. Konishi and M. Kurokawa, *Sen-I Gakkaishi (Engl. Transl.), 24*, 350 (1968). (b) S. A. Fossey, G. Nemethy, K. D. Gibson, and H. D. Scheraga, *Biopolymers, 31*, 1529 (1991). (c) D. L. Kaplan, S. J. Lombardi, W. S. Muller, and S. A. Fossey, in *Biomaterials: Novel Materials from Biological Sources* (D. Byron, Ed.), Stockton Press, New York, NY, 1991.

[11] The single-letter abbreviations of the amino acids are A = alanine, G = glycine, and E = glutamic acid.

[12] B. Lotz, A. Brack, and G. Spach, *J. Mol. Biol., 87*, 193 (1974). The silk I-like structure of poly(AG) was designated PLAG-II by Lotz et al., and the silk II-like structure of poly(AG) as PLAG-I. In retrospect, this notation is awkward; first because of the interchange of the Roman numerals I and II in comparison with the older silk notation (especially so since silk I can be

considered as a precursor to silk II and therefore there is a built-in logic to the silk notation), and second because the PL symbol is also the single-letter amino acid code for the ProLeu dimer. The PLAG-I/PLAG-II notation could create confusion situations in the description of polypeptides involving these amino acids. Thus, we have chosen to align the nomenclature of our two poly$(AG)_3EG$ structures with the two different silk structures rather than the PLAG notation. Thus, in summary: poly$(AG)_3EG$-I relates to silk I and PLAG-II [poly(AG)-II], and poly$(AG)_3EG$-II relates to silk II and PLAG-I [poly(AG)-I].

[13] H. Saito et al., *Macromolecules, 17*, 1405 (1984).